Computing specific intensity distributions for laser material processing by solving an inverse heat conduction problem

Annika Völl*[a], Jochen Stollenwerk[a,b], Peter Loosen[a,b]

[a]Chair for Technology of Optical Systems, RWTH Aachen University, 52056 Aachen, Germany
[b]Frauhofer Insitute for Laser Technology, Steinbachstraße 15, 52074 Aachen, Germany

ABSTRACT

Laser beam intensity distribution profiles for material processing techniques are most of the time restricted to be either of Gaussian or tophat shape. This often leads to different kind of problems especially at the edges of the laser-heated tracks, examples are energy losses or unnecessary overlaps. Thus, machining quality and process efficiency could be much improved by using application specific intensity profiles to generate optimal temperature distributions in the processed material. In this work, we present a numerical method to derive a specific intensity profile for a given temperature distribution. As this problem belongs to the set of inverse heat conduction problems, which are ill-posed, special regularization algorithms are needed. The only method to solve this inverse problem in reasonable time is the conjugate gradient method which we extend to the given problem of laser material processing applications. This method is an iterative approach where in each step the actual temperature distribution is calculated by using the finite element method. In general, the proposed method is applicable for materials with constant or temperature dependent coefficients, for static and dynamic distributions as well as for plane or complex geometries. However, restricting ourselves to plane geometries, intensity distributions that create tophat- or stepped temperature distributions on the plane surface of the processed material are derived and will be presented. In future work, we intend to verify these results using freeform optics as well as singly addressable V(E)CSEL arrays.

Keywords: laser heat treatment, conjugate gradient method, finite elements, laser application, beam shaping, optimization, beam profile

1. INTRODUCTION

For the last 50 years, laser heat treatment is increasingly replacing conventional methods of material processing. Especially through the local influence, the potential to be incorporated inline in a manufacturing process and the high energy efficiency, laser material processing has become a powerful tool which is already widely used in industry[1].

In laser material processing, extensive studies have been performed on many influencing parameters such as laser power, beam focus, feed speed, and spot size[2]. However, only very few publications can be found in literature that optimize the intensity profile within the beam spot. The intensity profile directly influences the induced temperature distribution in the material and this temperature profile lastly causes the material's transformations. Thus, a process can be much improved by using application specific intensity profiles.

Currently, tophat or Gaussian intensity profiles are used almost exclusively. Both beam profiles induce temperature distributions that have a maximum in the center and decrease at the edges (for the Gaussian beam this feature is more prominent). Consequently, positions in the center of the track are overheated while parts at the edges might not even be processed correctly. Additionally, the depth of the transformation is much higher in the center compared to the edges, often resulting in a characteristic lens shape of the transformed material[3,4]. Using specific intensity distributions which induce a predetermined temperature distribution in the material might therefore result in a higher offset between two parallel heated tracks and accordingly in higher process efficiency as well as productivity.

* annika.voell@tos.rwth-aachen.de, phone +49 241 8906-8369, fax +49 241 8906-121, www.tos.rwth-aachen.de

Among the very few methods published in literature, we did not find any that is generally applicable to the wide range of geometries, materials and temperature specifications used in laser material processing. Burger[5] derives a specific intensity profile that induces a homogeneous temperature distribution for laser hardening. However, the method has not been applied to other prescribed temperature fields. It is furthermore restricted to planar surfaces and neglects the temperature dependence of the material's thermo-physical properties. The method described by Kharkin[6], on the other hand, examines laser welding and furthermore suffers from a low number of parameters.

Mathematically, the problem of deriving the optimal intensity profile for a given intensity distribution is an inverse heat conduction problem (IHCP)[7]. There are several methods to solve an IHCP in one dimension. However, the Tikhonov regularization[8] turns out to be completely inefficient in three dimensions. Beck's function specification method[9], on the other hand, is not applicable to higher dimensions. The only method which successfully solves inverse heat conductions problems in three dimensions is the conjugate gradient method with adjoint problem[10,11]. Soemers, for example, implemented this method to analyze falling film experiments[12].

In this work, we apply the conjugate gradient method to derive application specific intensity distributions that generate a prescribed temperature field in laser heat treatment applications. The remainder is structured as follows: in section 2 we present the method to solve the IHCP for static distributions. Afterwards, in section 3, we present and analyze numerical results of this approach by showing intensity profiles that generate homogeneous or stepped temperature fields. Finally, in section 4, we discuss the results and sketch how the method is extended to dynamic distributions.

2. METHOD: AN IHCP FOR LASER MATERIAL PROCESSING

Consider a material with density ρ, thermal conductivity k, heat capacity c, and an absorption coefficient A. Let the material be processed with the intensity distribution I at feed speed $\vec{v}$. For static distributions, the heat conduction in the coordinate system of the laser beam can then generally be expressed via the heat conduction equation

$$-\nabla(k\,\nabla T) = -\vec{v}\rho c\nabla T \tag{1}$$

with either Neumann ($-k\vec{n}\nabla T = A \cdot I$) or Dirichlet ($T = T_S$) boundary conditions on the volume's surface (in the following we will call them $\partial\Omega_N$ and $\partial\Omega_D$). Here, ρ, c, and k might depend on position and temperature, and $T = T(x, y, z)$ is the temperature field which is induced by an intensity distribution $I = I(x, y, z)$. Furthermore, it is assumed that the radiation is absorbed at the material's surface which is modeled by the Neumann boundary condition.

Usually, if the heat conduction for laser material processes is investigated, the temperature field that is originating from a given intensity distribution is of interest. Here, however, it is the exact opposite. We prescribe parts of the temperature field that we want to induce, and we search for the related intensity distribution. Thus, we want to solve an *inverse* heat conduction problem. This, unfortunately, is known to be an ill-posed problem[8], for which special regularization methods are needed to stabilize the solution.

To solve the inverse problem, we extend an iterative approach which has originally been developed by Alifanov[10] and then been applied to several IHCPs by Özisik[11]. We assume, that we prescribed the temperature field at N discrete points. Similarly to other inverse problems, the method then iteratively minimizes the least squares sum

$$S = \sum_i (T_i - Y_i)^2 \tag{2}$$

where Y_i refers to the prescribed temperature profile at position x_i and T_i is the related temperature for a given intensity distribution I. Thus, by minimizing S we approach the optimal distribution I that induces the prescribed temperature field.

In the conjugate gradient method, an initial guess for I is assumed and this intensity distribution is then updated repetitively according to

$$I^{n+1} = I^n - \beta^n d^n \tag{3}$$

Here, d^n is a combination (a *conjugation*) of the previous update direction (we assume 0 for the first iteration) and the direction in which the least square sum decreases maximally (the direction of the gradient of S)

$$d^n = \nabla S(I^n) + \gamma^n d^{n-1} \tag{4}$$

The computation of the factors β^n and γ^n is done later on.

The difficult part now is to find an expression for ∇S. As a first step, assume I and T are known for a certain iteration and consider a small change in the intensity profile δI. By subtracting the heat conduction equation (1) for T from the one for the changed field $T + \delta T$, the difference in temperature δT can be derived by the so called *sensitivity* problem

$$-\nabla\big(\nabla(k(T)\delta T)\big) = -\vec{v}\nabla\left(\left(\rho(T)c(T) + \rho(T)\frac{\partial c}{\partial T}T + c(T)\frac{\partial \rho}{\partial T}\,T\right)\delta T\right) \tag{5}$$

with the boundary conditions $-\vec{n}\nabla(k(T)\delta T) = A \cdot \delta I$ on $\partial\Omega_N$ and $\partial \mathrm{T} = 0$ on $\partial\Omega_D$. Equation (5) is similar to equation (1) though it shall be noted that, although the parameters in equation (1) depend on its solution, this does not hold for equation (5). Here, the coefficients depend only on T, which is a known temperature field. Thus, the coefficients may vary with position, but they are not dependent on the solution of (5).

To obtain ∇S, equation (1) is regarded as a constraint on equation (2) which can be respected via a Lagrange multiplier λ

$$S = \sum_i (T_i - Y_i)^2 + \int_V \lambda(x,y,z)(-\nabla(k\,\nabla T) + \vec{v}\,\nabla(\rho c T))dV \tag{6}$$

Now, denoting $\tilde{S} = S + \delta S$, calculating $\tilde{S}(I + \delta I) - S(I)$, and using the sensitivity problem (5) as well as integration by parts on the boundaries yields for δS

$$\delta S(\delta I) = -2\sum_i (Y_i - T_i)\,\delta T + \int_\Omega \lambda\vec{n}\vec{v}\left(\rho c + \rho\frac{\partial c}{\partial T}T + c\frac{\partial \rho}{\partial T}T\right)\delta T d\Omega - \int_V \nabla\lambda\vec{v}\left(\rho c + \rho\frac{\partial c}{\partial T}T + c\frac{\partial \rho}{\partial T}T\right)\delta T dV - \int_V k\nabla(\nabla\lambda)\delta T dV - \int_{\partial\Omega_D}\vec{n}\nabla\lambda k\delta T d\Omega + \int_{\partial\Omega_N}\lambda A\delta I d\Omega \tag{7}$$

Since the minimum of S cannot depend on δT, the sum of the terms containing this expression should equal to zero. This then yields the so call *adjoint* problem for λ

$$-k\nabla(\nabla\lambda) = -2(Y_i - T_i)\delta(x - x_i)\delta(y - y_i)\delta(z - z_i) - \vec{v}\left(\rho c + \rho\frac{\partial c}{\partial T}T + c\frac{\partial \rho}{\partial T}T\right)\nabla\lambda \tag{8}$$

with boundary conditions

$$\vec{n}\vec{v}\left(\rho c + \rho\frac{\partial c}{\partial T}T + c\frac{\partial \rho}{\partial T}T\right)\lambda - \vec{n}k\nabla\lambda = 0 \tag{9}$$

on $\partial\Omega$. Thus, if λ satisfies the adjoint problem, δS is given by

$$\delta S = \int_{\partial\Omega_\mathrm{N}} \lambda A\delta I d\Omega \tag{10}$$

On the other hand, $\delta S(\delta \mathrm{I}) = \sum_j \nabla S_j\,\delta I_j$, from which it follows that

$$\nabla S_j = \int_{\partial\Omega_N[I_j]} \mathrm{A}\lambda d\Omega \tag{11}$$

where $\partial\Omega_N[I_j]$ refers to that part of the boundary where I_j is inflicted.

As we now have computed δT and ∇S, we apply standard formulae[10,11] to compute β^n and γ^n

$$\beta^n = \frac{\sum_i (T_i - Y_i)\delta T(x_i, y_i, z_i)}{\sum_i \delta T(x_i, y_i, z_i)^2} \tag{12}$$

$$\gamma^n = \frac{\sum_i \left(\nabla S(I^n)\right)_i \left(\nabla S(I^n) - \nabla S(I^{n-1})\right)_i}{\sum_i \left(\nabla S(I^{n-1})\right)_i^2} \tag{13}$$

Here, the *Polak-Ribière* scheme[13] is used to compute the conjugation factor γ^n. With this, the description of the algorithm nearly is complete. It is only missing a few more notes.

The direct problem (1), the sensitivity problem (5), and the adjoint problem (8) are all partial differential equations and can thus be solved using standard solution methods. For our examples in section (3) we implemented finite element schemes using the *deal.II* library[14].

One word shall be stated concerning the regularization. For ill-posed problems, regularization usually is necessary to smooth oscillations arising from unphysical input such as measurement errors to the input data. In the conjugate gradient method, regularization is obtained by fixing the number of iterations N_{iter} which may either be achieved through the *discrepancy principle*[10,11] or the *l-curve* approach[15]. Here, however, we prescribe a temperature field that is error-free and otherwise physical. Thus, as in other optimization methods, we obtain more consistent results if the number of iterations is higher and we choose N_{iter} according to the requested accuracy level. It should be noted, though, that the number of iterations increases the running time. Thus, finding an optimal value for N_{iter} always means balancing accuracy and running time.

Putting it all together, the algorithm presented in Figure 1 solves the inverse heat conduction problem to obtain an application specific intensity distribution for laser material processing. Figure 1 also displays the most advantageous property of the conjugate gradient method. In each cycle, only three solutions are required from the FEM program. This extremely reduces the running time compared to other minimization methods that usually need calculations of the Hessian matrix. Indeed, the conjugate gradient method is the only approach in literature which can handle the problem in reasonable time.

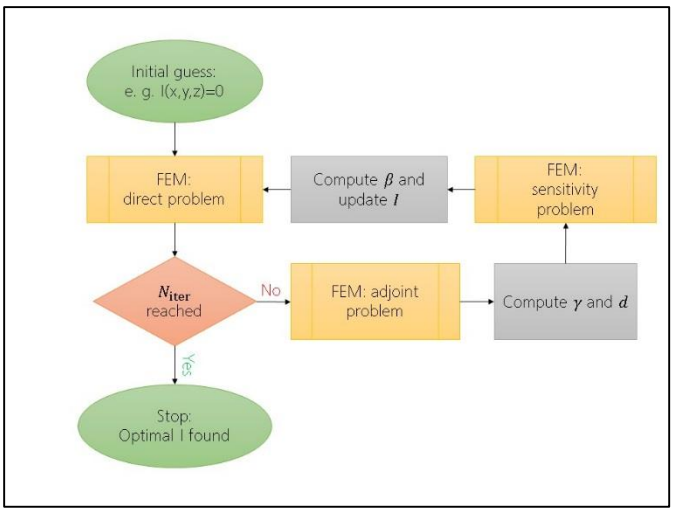

Figure 1: Flowchart of the algorithm to compute application specific intensity distributions. In each iteration, only 3 FEM solutions are required (yellow boxes with doubled lines)

3. NUMERICAL RESULTS

The method presented in the previous section is applicable to nearly all possible geometries as well as constant or temperature dependent material properties. However, in the following, we restricted ourselves to planar surfaces, but we accounted for the temperature dependence of the material properties.

For the test cases, we considered a block of steel out of 100Cr6[16], which is a commonly used material for a wide range of technical applications. We considered the volume $-10\ mm < x < 10\ mm$, $-10\ mm < y < 10\ mm$, and $0\ mm < z < 4\ mm$ and assumed that the surface at $z = 0\ mm$ is heat treated (see Figure 2). Therefore, we applied the Dirichlet boundary condition $T = 20°C$ on the surface $y = -10\ mm$, the Neumann boundary condition $-k\frac{dT}{dz} = A \cdot I$ on the surface $z = 0$ to simulate the surface absorption, and adiabatic boundary conditions on all other boundaries ($-k\vec{n}\nabla T = 0$). We chose $\vec{v} = (0, -0.1, 0)^T\ m/s$ and a spot size of $10\ mm\ x\ 10\ mm$, which are typical values for several laser heat treatment applications. Furthermore, an absorption coefficient of 0.5 is assumed. For the finite element simulations, we assumed an equidistant mesh with spacing $dx = 0.25\ mm$, $dy = 0.25\ mm$, and $dz = 0.25\ mm$ and we used first order elements. We calculated the intensity distribution $I = I(x, y)$ with the same resolution. Additionally, we fixed the number of iterations to be $N_{\mathrm{iter}} = 30$ which yields satisfactory results.

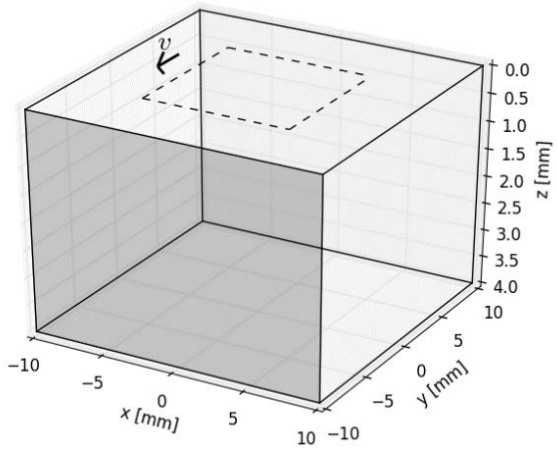

Figure 2: Geometry used for the test cases. We considered a block of steel (solid lines) which is processed at feed speed $\vec{v}$. Dirichlet boundary conditions are applied to the surface at $y = -10\ mm$ (transparent plane) and otherwise Neumann conditions are assigned. Apart from the square on the top (dotted lines) representing the processed surface, the Neumann boundary condition value is 0 to simulate adiabatic boundary conditions.

To test our algorithm, we computed the intensity profiles for two different prescribed temperature distributions. As stated above, specific intensity distribution profiles shall reduce negative side effects that are typical for tophat- or Gaussian profiles. To reduce the overheating in the center of the heated track and at the same time increase the temperature at its edges, we chose a uniform temperature distribution as our first test case. Burger[5] showed that, at least for laser hardening applications, the highest possible amount of the beam's energy will thus be injected into the processed material. Therefore, for the first test case, we predefined $Y_i = 750$°C for $N = 40\ 000$ regularly spaced points in the square area $-5\ mm < x < 5\ mm$, $-5\ mm < y < 5\ mm$, and $z = 0\ mm$.

Figure 3 shows a greyscale plot of the intensity distribution which we obtained with the method presented in section 2. The distribution's shape (which is in agreement with previous results[5]) is very irregular with a high peak at the front edge and middle sized elevations at the side edges. However, it is rather straightforward to explain this shape. At first, the material is heated rather instantly for which a high intensity is needed. Afterwards, only a small amount of energy needs to be injected to keep the temperature constant. Furthermore, the elevations at the side edges arise as a consequence of thermal diffusion. Altogether, the total power needed for this $10\ mm\ x\ 10\ mm$ spot is $6484\ W$, which is a completely reasonable value in many laser heat treatment processes[2]. The corresponding temperature distribution is very homogeneous with less then 3 % variation (Figure 4). The remaining oscillations mainly occur at the edges and are in general diminished if a higher number of iterations is chosen. Additionally, a finer FEM grid should further improve the results.

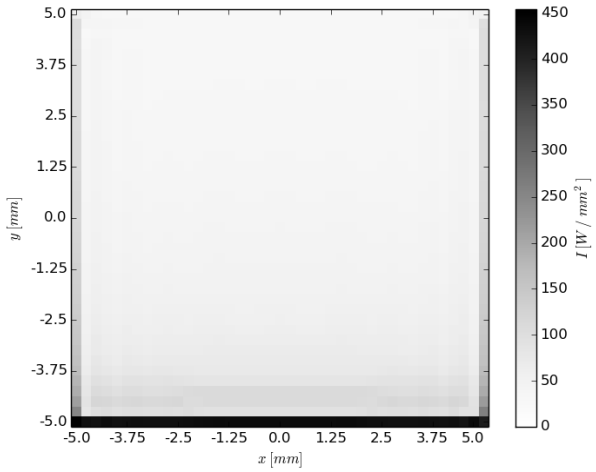

Figure 3: Intensity which induces a homogeneous temperature distribution on the surface of steel out of 100Cr6. Spotsize, discretization and feed speed are given in the text. The total power needed is $6484\ W$.

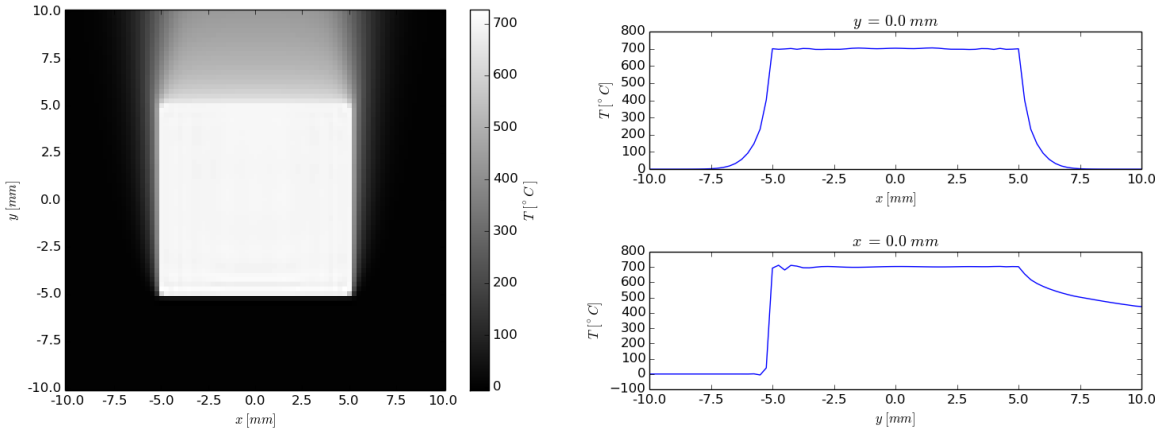

Figure 4: Achieved temperature distribution obtained with the intensity distribution from Figure 3. Left: Top-View. Right: Cross sections through the origin. The variation of the temperature lies below 3 %.

In some applications, the abrupt jump in temperature induces material strains and therefore the heating should occur gradually or in several steps[17]. To simulate such processes, our second test case is a temperature field which is composed of three homogeneous profiles with increasing values for the temperatures. In this way, surface points undergo three smaller temperature changes ($20\ °C \rightarrow 250\ °C \rightarrow 500\ °C \rightarrow 750\ °C$) which reduces the strains to the material. Here, we chose the same N_i input positions as in the first test case and assigned the temperature values accordingly.

For this second test case, the algorithm from section 2 produced the intensity distribution shown in Figure 5. In light of the results of the previous paragraph, this profile should not surprise. As the temperature field comprises three homogeneous distributions, the corresponding intensity profile is likewise composed of three distributions similar to the one in Figure 3. Indeed, each of these three profiles accounts for one step in the temperature distribution. The resulting temperature field which is displayed in Figure 6 shows a high homogeneity in each step with variations below 5 %.

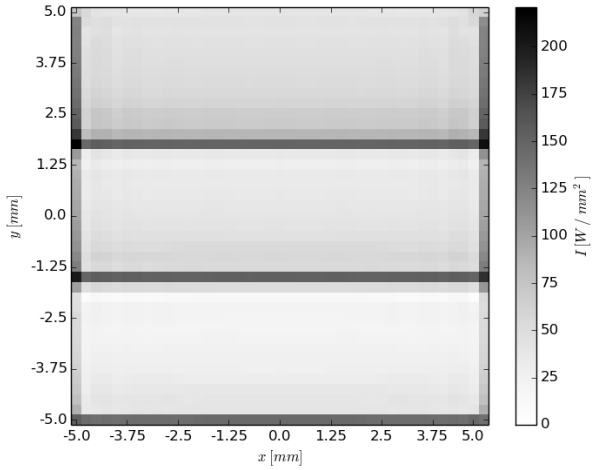

Figure 5: Intensity which induces a stepped temperature distribution on the surface of steel out of 100Cr6. Spotsize, discretization and feed speed are given in the text. The total power needed is 5520 W.

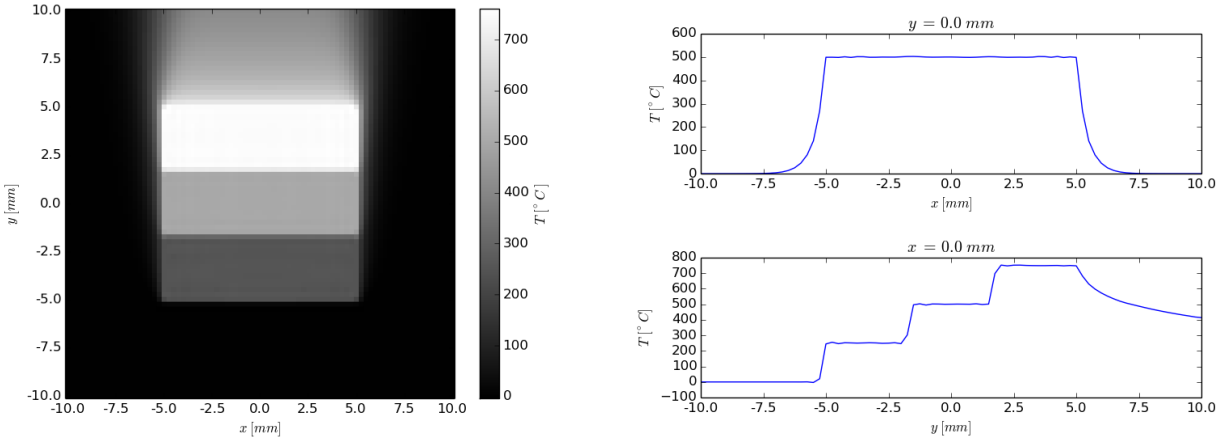

Figure 6: Achieved temperature distribution obtained with the intensity distribution from Figure 5. Left: Top-View. Right: Cross sections through the origin. The variation of the temperature in the three section lies below 5 %.

4. DISCUSSION & OUTLOOK

In this work, we presented an inverse method to calculate application specific intensity distributions for laser heat treatment applications. Using a combination of the conjugate gradient method with FEM, we derived showcase intensity distributions that create homogeneous or stepped temperature profiles on a planar surface of a block of steel out of 100Cr6. The obtained intensity profiles are in agreement with previous results and it is easy to understand their features.

Although there are some other methods to derive specific intensity profiles, the presented approach stands out because of its efficiency and its general applicability. As stated in section 2, only three FEM solutions are needed for one iteration of the conjugate gradient method. Furthermore, the method already accounts for complex geometries and the temperature dependence of the material's properties.

Additionally, it is very straightforward to extend the presented method to dynamic distributions and volumetric heat sources. Time-dependent heat conduction is modeled by adding the term $\rho c \frac{\partial T}{\partial t}$ on the left hand side of equation (1). A similar approach to the one from section 2 then leads to augmented equations for the sensitivity as well as the adjoint problem. However, there is a delicacy concerning the adjoint problem. As the integration by parts for the time-dependent term results in a condition for the final time value of the simulation $t = t_f$, the transformation $\tau = t - t_f$ is necessary to enable the use of FEM. Volumetric heat sources, on the other hand, are represented by simply adding their value $+s$ on the right hand side of equation (1). This then also leads to further adapted equations for the sensitivity and the adjoint problem.

The next step is to actually implement these intensity distributions in an experimental setup and use them for different kinds of laser heat treatment. To create specific intensity distributions, we suggest either the use of freeform optics[18] or of singly addressable V(E)CSEL arrays[19,20]. Both enable the forming of highly irregular intensity distributions. It will be interesting to see how much machining quality and process efficiency can be improved by using application specific intensity distributions.

5. ACKNOWLEDGEMENTS

This work was funded by the German Federal Ministry of Education and Research (BMBF) under grant number 13N13476. Furthermore, we acknowledge useful discussions with Rolf Wester and Norbert Pirch.

REFERENCES

[1] Poprawe, R., [Tailored Light 2], Springer, Berlin Heidelberg, 1-4 (2011).
[2] Poprawe, R., [Tailored Light 2], Springer, Berlin Heidelberg, 173-240 (2011).
[3] Steen, W. M., Courtney, C., "Surface heat treatment of EnS steel using a 2kW continuous-wave CO2 laser," Metals Technology 6(1), 456-462 (1979).
[4] Gassman, R. C., "Laser cladding with (WC + W2C)/Co-Cr-C and (WC +W2C)/Ni-B-Si composites for enhanced abrasive wear resistance," Mater Sci Tech Ser 12(8), 691-696(1996).
[5] Burger, D., [Beitrag zur Optimierung des Laserhärtens], PhD Thesis, University of Stuttgart (1988).
[6] Karkhin, V. A., Plochikhine, V. V., Bergmann, H. W., "Solution of inverse heat conduction problem for determining heat input, weld shape, and grain structure during laser welding," Sci Technol Weld Joi 7(4), 224-231(2002).
[7] Beck, J. V., Blackwell, B, St Clair Jr, C. R., [Inverse heat conduction: ill-posed problems], J. Wiley and Sons, New York 1-39(1985).
[8] Tikhonov, A. N., Arsenin, V. Ya., [Solution of ill-posed problems], VH Winston & Sons, Washington, DC (1977).
[9] Beck, J. V., Blackwell, B, St Clair Jr, C. R., [Inverse heat conduction: Ill-posed problems], J. Wiley and Sons, New York 267-280(1985).
[10] Alifanov, O. M., [Inverse heat transfer problems], Springer, Berlin, Heidelberg (1994).
[11] Özisik, M. N., Orlande, H. R. B. [Inverse heat transfer], Taylor & Francis, New York (2000).
[12] Soemers, M., [Numerical methods for the solution of a three-dimensional anisotropic inverse heat conduction problem], PhD Thesis, RWTH Aachen (2008).
[13] Polak, E., Ribière, G., "Note sur la convergence de methods de directions conjuguées," Revue française d'informatique et de recherché opérationnelle, série rouge 3(1), 35-43(1969).
[14] Bangerth, W., Hartmann, R., Kanschat, G., "deal.II – a general-purpose object-oriented finite element library," ACM T Math Software 33(4), 27(2007).
[15] Hansen, P. C., O'Leary, D. P., "The use of the L-curve in the regularization of discrete ill-posed problems," SIAM J. Sci. Comput. 14(6), 1487-1503(1993).
[16] Spittel, M., Spittel, T., [Metal Forming Data of Ferrous Alloys – deformation behavior], Springer, Berlin Heidelberg, 552-557(2009).
[17] www.doerrenberg.de/uploads/tx_c1x1downloads/1.2379_de.pdf
[18] Bäuerle, A., Bruneton, A., Wester, R., Stollenwerk, J., Loosen, P., "Algorithm for irradiance tailoring using multiple freeform optical surfaces," Opt. Express 20, 14477-14485 (2012).

[19] Moench, H., Deppe, C., Derra, G., Gronenborn, S., Gu, X., Heusler, G., Kolb, J., Miller, M., Pekarski, P., Pollman-Retsch, J., Pruijmboom, A., Weichman, U., "High power VCSEL systems and applications", Proc SPIE 9348-32, 1-10 (2015).
[20] Okhotnikov, O. G. (Ed.), [Semiconductor disk lasers – Physics and Technology], Wiley-VCH, Berlin (2010).